Photoacoustics 1 (2013) 3–8

Contents lists available at SciVerse ScienceDirect

Photoacoustics

journal homepage: www.elsevier.com/locate/pacs

Research Article

Multispectral optoacoustic tomography of myocardial infarction

Adrian Taruttis [1,2,*], Moritz Wildgruber [3], Katja Kosanke [3], Nicolas Beziere [1,2], Kai Licha [5], Rainer Haag [6], Michaela Aichler [4], Axel Walch [4], Ernst Rummeny [3], Vasilis Ntziachristos [1,2]

[1] Institute for Biological and Medical Imaging, Helmholtz Zentrum München, Ingolstädter Landstr. 1, 85764 Neuherberg, Germany
[2] Chair for Biological Imaging, Technische Universität München, Ismaninger Str. 22, 81675 München, Germany
[3] Department of Radiology, Klinikum Rechts der Isar, Technische Universität München, Ismaninger Str. 22, 81675 München, Germany
[4] Research Unit Analytical Pathology - Institute for Pathology, Helmholtz Zentrum München, Ingolstädter Landstr. 1, 85764 Neuherberg, Germany
[5] mivenion GmbH, Robert-Koch-Platz 4, 10115 Berlin, Germany
[6] Institut für Chemie und Biochemie, Freie Universität Berlin, Takustr. 3, 14195 Berlin, Germany

ARTICLE INFO

Article history:
Received 26 July 2012
Received in revised form 14 November 2012
Accepted 14 November 2012

Keywords:
Myocardial infarction
Optical imaging
Optoacoustic imaging

ABSTRACT

Objectives: To investigate the feasibility of a high resolution optical imaging strategy for myocardial infarction.
Background: Near-infrared approaches to imaging cardiovascular disease enable visualization of disease-associated biological processes *in vivo*. However, even at the scale of small animals, the strong scattering of light prevents high resolution imaging after the first 1–2 mm of tissue, leading to degraded signal localization.
Methods: Multispectral optoacoustic tomography (MSOT) was used to non-invasively image myocardial infarction (MI) in a murine model of coronary artery ligation at resolutions not possible with current deep-tissue optical imaging methods. Post-MI imaging was based on resolving the spectral absorption signature of a dendritic polyglycerol sulfate-based (dPGS) near-infrared imaging agent targeted to P- and L-selectin.
Results: *In vivo* imaging succeeded in detection of the agent in the injured myocardium after intravenous injection. The high anatomic resolution (<200 μm) achieved by the described method allowed signals originating in the infarcted heart to be distinguished from uptake in adjacent regions. Histological analysis found dPGS signal in infarcted areas, originating from leukocytes and endothelial cells.
Conclusions: MSOT imaging of myocardial infarction provides non-invasive visualization of optical contrast with a high spatial resolution that is not degraded by the scattering of light.

1. Introduction

In vivo optical imaging in the near-infrared (NIR) spectrum plays a significant role in cardiovascular research. Intravascular molecular imaging with a NIR fluorescence (NIRF) catheter has been demonstrated as a highly promising method for detecting protease activity in atherosclerotic plaques [1,2]. Non-invasive optical imaging of processes implicated in cardiovascular disease has also been reported. For example, visualization of macrophage infiltration using fluorescent nanoparticles [3] and investigations of monocyte recruitment for infarct healing [4] have been performed using Fluorescence Molecular Tomography (FMT). However, optical imaging methods are limited in performance by scattering, which degrades the spatial resolution and overall accuracy at increased penetration depths [5]. Optoacoustic imaging, in particular Multispectral Optoacoustic Tomography (MSOT) offers a way around this problem by producing images of specific optical contrast at ultrasound resolutions.

Optoacoustic imaging is based on the optoacoustic (photoacoustic) effect, whereby short (usually nanosecond range) pulses of light that are absorbed in tissue give rise to broadband ultrasound waves, which can be detected non-invasively [5]. Since ultrasound scatters orders of magnitude less than light in tissue, optoacoustic methods can offer high-resolution optical images in tissues up to several centimeters deep. The signal observed on optoacoustic images is directly proportional to the local absorption coefficient. By applying multiple excitation wavelengths and tomographic signal detection, MSOT can provide images of specific chromophores (absorbers) based on their unique spectra [6–8]. Spectral unmixing methods have been shown to resolve oxygenated and deoxygenated

* Corresponding author at: Technische Universität München, Lehrstuhl für Biologische Bildgebung, Ismaninger Str. 22, 81675 München, Germany.
Tel.: +49 89 3187 3852 (assistant); fax: +49 89 3187 3008.
E-mail address: adrian.taruttis@mytum.de (A. Taruttis).

2213-5979
http://dx.doi.org/10.1016/j.pacs.2012.11.001

states of hemoglobin [9] and the bio-distribution of exogenously administered photo-absorbing agents including organic dyes [7,10] and nanoparticles [11,12]. Applied to cardiovascular imaging, MSOT has demonstrated anatomical visualization of the mouse heart and blood vessels [13]. Motion correction techniques for multi-wavelength excitation [14] have also been developed, allowing high-resolution spectral unmixing of the beating heart. In addition, MSOT detection of molecular imaging agents relevant to cardiovascular disease was demonstrated by resolving matrix–metalloproteinase (MMP) activity in human atherosclerotic plaque specimens [15]. *Ex vivo* optoacoustic imaging of excised mouse hearts has demonstrated visualization of infarcted regions with reduced absorption compared to healthy tissue, resulting from reduced hemoglobin concentration due to ischemia [16].

In this study, we investigated the previously undocumented ability of MSOT to image myocardial infarction *in vivo* using an exogenously administered targeted optical agent. Specifically, we hypothesized that the detection of an inflammation-targeted NIR imaging agent based on dendritic polyglycerol sulfates (dPGS) is possible in mice *in vivo* and that it could be imaged within infarcted myocardium in high resolution. Results were contrasted to histological analysis and macroscopic cryosection NIRF imaging of the dPGS distribution within the infarcted myocardium, serving as the gold standard.

2. Methods

2.1. Animal handling

All procedures involving animals were approved by local subcommittee on animal research. We used a total of 15 adult female C57BL/6 mice in this study. The mice were anesthetized for all surgical and imaging procedures by general inhalation anesthesia (Isofluorane 1.5–2.5% vol., plus 2 l O_2). We induced myocardial infarction by permanent ligation of the left anterior descending artery (LAD) leading to a transmural infarct as previously described [3].

2.2. Imaging agent

Dendritic polyglycerol sulfates (dPGS) are highly branched structures with a polyanionic sulfate surface that can interact *via* a multivalent binding mechanism with basic protein motifs. It has been shown that dPGS binds to P- and L-selectin [17], and imaging studies with NIR conjugates proved selective accumulation in inflamed joints [18] in a preclinical model of arthritis.

The dPGS-NIR dye conjugate was synthesized by anionic polymerization of glycidol, modification with an aliphatic azido-linker chain followed by the sulfation reaction. To this linker, NIR dye (6S-ICG propargyl; mivenion GmbH, Berlin, Germany) was conjugated followed by HPLC purification yielding dPGS-NIR with a mean dye-to-polymer ratio of 3 and an average molecular weight of 19000 Da. Absorption maxima in PBS were 710 and 795 nm, fluorescence emission maximum 810 nm. The fluorescence quantum yield in water was below 1% due to intramolecular quenching. The high absorption per polymer due to multiple dye attachment, the absorption peak around 800 nm, and the low quantum yield provide a NIR agent with favorable properties for detection by MSOT based on absorption.

For *ex vivo* histology, dPGS-ICC dye was used. This conjugate is the structural analog of dPGS-NIR employing a fluorophore with visible fluorescence (ICC propargyl: 550 nm absorption, 570 nm emission peak, mivenion GmbH) enabling detection in standard fluorescence microscopes [18]. In addition, the corresponding nonspecific agent based on the same polymer but without sulfation, dPG-ICC, was applied for control purposes.

2.3. MSOT imaging system

All MSOT imaging experiments were performed using a real-time imaging system that has been described previously [13,19]. Optical excitation was provided by a Q-switched Nd:YAG laser with a pulse duration around 10 ns and repetition rate of 10 pulses/s, which pumped an optical parametric oscillator (OPO) with a wavelength tuning range in the near-infrared from 700 nm to 950 nm. Light was delivered by a fiber bundle divided into 10 output arms to illuminate the subject being imaged from multiple angles around the imaging plane. Optoacoustic signals were measured using a 64-element concave (172° active arc) transducer array with a central frequency of 5 MHz. One transverse slice was acquired from each laser pulse, resulting in a frame-rate of 10 Hz. The acquisition time per frame is 32 μs for a 2 cm field of view (time taken for optoacoustic signals to propagate to the transducer array). Image reconstruction took less than 100 ms, allowing imaging in real-time. The in-plane resolution is in the range of 150–200 μm. During imaging, the fiber bundle outputs and transducer array were stationary, while the subject could be translated to capture different transverse slices. Measurements took place in a temperature-controlled water bath for acoustic coupling. An animal holder with a thin polyethylene membrane prevented direct contact between the mouse and the water.

2.4. Phantom imaging

To verify optoacoustic detection of the dPGS-NIR spectrum under controlled conditions, we imaged a solution of the agent included in the center of a cylindrical, light-scattering phantom.

A stock solution of the agent was prepared by adding 1% Albumin (Carl Roth, Karlsruhe, Germany) by weight to 250 nM dPGS-NIR in PBS. The Albumin was included to simulate *in vivo* conditions for the agent. For use as a standard of reference, we recorded the extinction spectrum of dPGS-NIR in a spectrometer (USB2000 VIS-NIR, Ocean Optics, Dunedin, Florida). We then performed phantom measurements for validation of MSOT detection of the dPGS-NIR absorption profile. The phantom consisted of 1.3% by weight of Agar (Sigma–Aldrich, Saint Louis, Missouri) molded into a cylinder of 2 cm diameter. 6% by volume of Intralipid 20% emulsion (Sigma–Aldrich) was added to the solution to obtain a background reduced optical scattering coefficient $\mu_{s'} \approx 10\ \mathrm{cm}^{-1}$. A plastic tube of 3 mm inner diameter containing the stock solution of dPGS-NIR was included at the center of the cylinder. Phantom imaging was performed in the same MSOT setup as the *in vivo* experiments. We applied excitation wavelengths from 690 nm to 900 nm in steps of 5 nm. For each wavelength we recorded and averaged optoacoustic signals from 50 frames (laser pulses).

2.5. Experimental protocol for in vivo MSOT

Mice were imaged on day 2 following myocardial infarction, a time point corresponding to a first peak of leukocyte influx in the injured myocardium [20,21]. Isofluorane anesthesia was applied for the duration of the experiments. Prior to MSOT imaging, hair was removed from the chest region using chemical depilation. A catheter was then inserted into the tail vein and the mice were placed in the prone position in the MSOT imaging system. A volume of interest ranging from the liver to the heart was selected by inspection of live MSOT images. The following 8 excitation wavelengths were selected for correspondence with the major turning points in the absorption spectra of the dPGS-NIR and hemoglobin: 710 nm, 730 nm, 760 nm, 790 nm, 800 nm, 820 nm, 850 nm, 900 nm. For each wavelength we recorded 100 individual frames, that is, 100 laser pulses or 10 s. At each time point, the region of interest was scanned with a pitch of 1 mm. Imaging was

performed before injection, directly after injection, and 1 h and 2 h after injection. The injected dose of dPGS-NIR was 8 mg/kg body weight (i.v.).

2.6. MSOT Image reconstruction and analysis

For *in vivo* MSOT measurements, motion binning was applied to all acquired frames [14]. In this step, the 100 frames recorded for each wavelength were separated into 3 different clusters corresponding to respiration, ventricular systole, and diastole. This clustering was performed by a *k*-means algorithm based on manually selected seed images for each phase. Subsequently, the mean images for each cluster, representing deblurred images for each phase, were used for further processing and analysis. For isolation of image contributions from dPGS-NIR, independent component analysis (ICA) was applied [22]. This algorithm separates the multispectral data into images comprising a set of maximally statistically independent source components. The source component corresponding to the unique absorption spectrum of dPGS-NIR (Fig. 1) was in each case selected from the ICA results by inspection. We performed analysis of the changes in signal intensity over time by first manually selecting a region corresponding to the entire heart, and subsequently automatically segmenting those pixels for each time point where the signal corresponding to dPGS-NIR was higher than twice the standard deviation from the mean.

2.7. Ex vivo *macroscopic and histological validation*

To validate the dPGS-NIR distribution imaged by MSOT, we performed *ex vivo* fluorescence cryoslicing imaging (FCSI) [23]. This method provides slice images in the same orientation (transverse plane) and at the same scale as MSOT, showing both anatomy (color) and dPGS-NIR distribution (NIRF). To this end, the same mice imaged by MSOT were euthanized by Ketamine overdose after the last imaging time point and then frozen at −80 °C embedded in optimal cutting temperature compound. They were subsequently sliced in a cryotome fitted with a multispectral fluorescence imaging system. Color as well as fluorescence images to detect dPGS-NIR were recorded at 250 μm intervals.

Histological analysis was applied to hearts harvested from the same model used for MSOT imaging to validate the specific distribution of dPGS in the context of myocardial infarction at a microscopic scale. dPGS-ICC was employed for histology as a substitute for dPGS-NIR, allowing more sensitive microscopic detection by visible fluorescence light emission. dPG-ICC was used as a nonspecific control agent in further animals. The experimental protocol was the same as for *in vivo* imaging: mice were injected with dPGS-ICC or dPG-ICC on day 2 following myocardial infarction and sacrificed 2 h following injection. Following resection, the hearts were immediately frozen in liquid nitrogen. The frozen hearts were cut into serial coronal sections of 12 μm thickness. Slices were stained with hematoxylin and eosin stain (H&E) or used for fluorescence microscopy. Fluorescence images were captured using an Axio Imager Z1 upright microscope system (Carl Zeiss, Oberkochen, Germany). The fluorescent agents were detected with a 43 HE DsRed filter set (Carl Zeiss). Nuclei were identified with Hoechst 33342 (filter set 49 DAPI, Carl Zeiss).

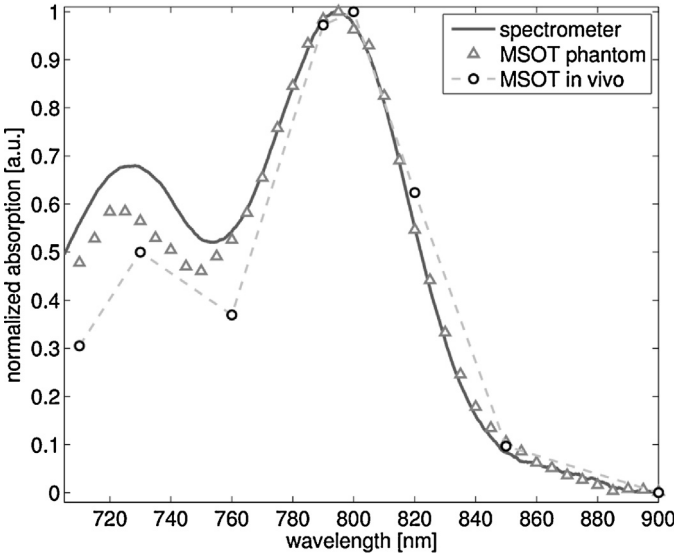

Fig. 1. dPGS-NIR absorption spectrum characterized in spectrometer (solid line), by optoacoustic phantom measurements (triangles) and by MSOT *in vivo* (circles). The values are all given relative to their peaks.

3. Results

3.1. Agent spectrum

Fig. 1 depicts the dPGS-NIR spectrum measured in a spectrometer and detected optoacoustically both in phantom experiments and *in vivo*. The peak optical absorption coefficient of the solution measured by the spectrometer was 0.3 cm^{-1} at 790 nm. The spectrum is characterized by a rapid drop in absorption to values less than 10% of the peak by 900 nm. The MSOT-derived spectrum closely matches the absorption spectrum measured by the spectrometer. This result is expected, since the optoacoustic signal amplitude is proportional to the local absorption coefficient, and confirms also the effectiveness of the unmixing algorithm (ICA) applied *in vivo*.

3.2. In vivo *detection by MSOT*

Inspection of the high-resolution MSOT images reveals anatomical structures including the anterior myocardium of the left and right ventricle (Fig. 2a and b). Endogenous tissue contrast, which is largely derived from light absorption by hemoglobin, is lower in the infarct region than elsewhere in the myocardium, attributed to a reduced local hemoglobin concentration. MSOT provided multispectral detection of dPGS-NIR in the injured myocardium *in vivo* (Fig. 2b), as validated *ex vivo* by NIRF on a corresponding cryosection (Fig. 2d). The agent was additionally detected both by MSOT and cryosection NIRF in the region of surgical thoracotomy. Accumulation in the scar is likely to be a result of post-surgery wound healing which is also characterized by an increased selectin expression and influx of leukocytes into the damaged tissue.

MSOT measurements at multiple time points post-injection provide information on the pharmacokinetic profile of the agent accumulation in the infarcted myocardium (Fig. 3). By taking the mean of the pixels where the single intensity from dPGS-NIR was more than twice the standard deviation from the mean for the entire heart, we found an increase in dPGS signal strength in the injured myocardium between the 15 min and 1 h time points, and a further slight increase between the 1 h and 2 h time points (Fig. 3d). Imaging time points prior to injection resulted in no detected spectral source components corresponding to dPGS-NIR, thus resulting in a baseline value of zero in the absence of the agent.

3.3. Histology

Areas of myocardial infarction were identified according to established histopathological criteria. Analysis of histological images from H&E stained slices showed large infarcted regions (Fig. 4a). In contrast to vital myocardial tissue, tissue in the area of

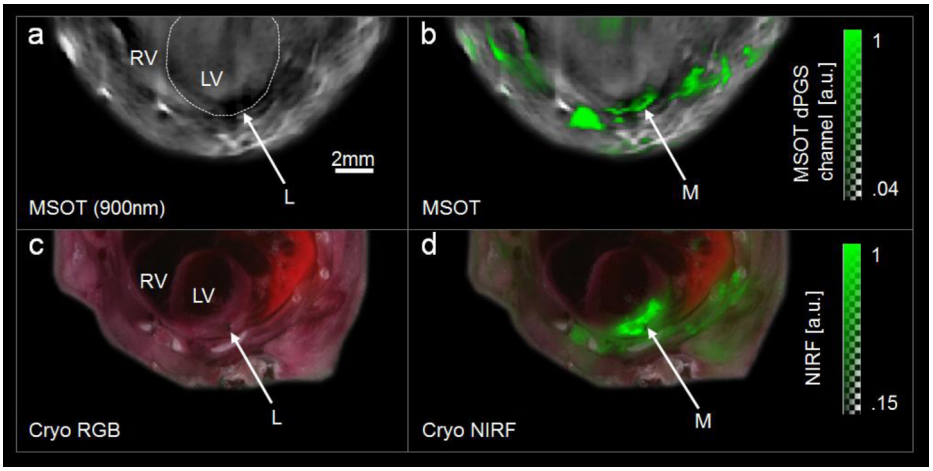

Fig. 2. Transverse slice images through site of ligation in mouse model of myocardial infarction. (a) Optoacoustic image taken at 900 nm. White dotted line indicates the left ventricle. L-region of ligation. RV-right ventricle, LV-left ventricle. Note the dark area around the ligation caused by reduced hemoglobin concentrations. (b) MSOT image. Spectrally unmixed signal from dPGS-NIR (green) superimposed on optacoustic image taken at 900 nm. M-infarcted myocardium. (c) Color photograph of corresponding cryosection (*ex vivo*) for validation. The ligation is visible. Labels the same as in (a). (d) Near infrared fluorescence (NIRF, green) from dPGS-NIR superimposed on color photograph of cryosection. dPGS-NIR is found in the infarcted myocardium as well as regions in the thoracic wall injured during surgery.

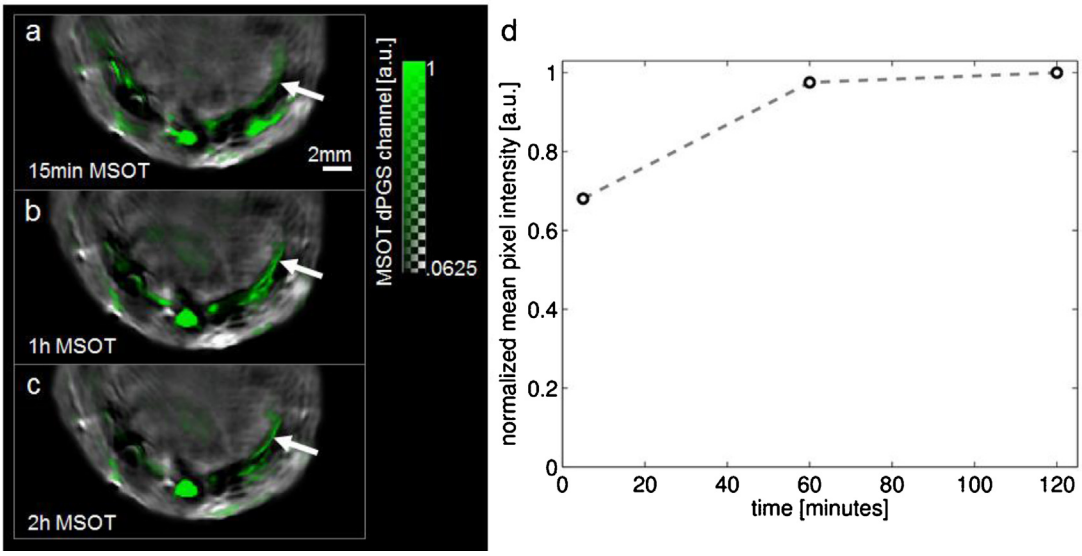

Fig. 3. Transverse slices over time through the chest of a mouse at day 2 following myocardial infarction. (a) MSOT image recorded 15 min after injection showing dPGS-NIR signal superimposed in green over image taken at 900 nm. Arrow indicates site of infarction. (b) 1 hour after injection. (c) 2 h after injection. (d) Mean pixel intensity of MSOT dPGS-NIR channel in pixels more than 2 standard deviations above the mean for the entire heart.

myocardial infarction was histopathologically characterized by a loss of nuclei and striation, increased infiltration of leukocytes and disintegration of dead muscle fibers (Fig. 4a). On a larger scale, fluorescence from dPGS-ICC was observed in the infarcted regions predominantly from the penumbral (border) zones (Fig. 4b). dPGS-ICC fluorescence was also found to originate from endothelial cells of blood vessels (Fig. 4c and d) and from leukocytes (Fig. 4e and f) in close association with the infarcted area, which are known to express P- and L-selectin respectively [24,25]. The images are thus consistent with targeting of dPGS to P- and L-selectin as previously described in models of arthritis [17,18]. In samples treated with the nonspecific control agent, dPG-ICC, no signal was observed (Fig. 4g and h).

4. Discussion

In this report we demonstrated *in vivo* MSOT imaging of murine myocardial infarction using a selectively targeted optical contrast agent. A spatial resolution below 200 μm is attained at penetration depths of several millimeters, which is not possible using conventional optical imaging [5]. As a comparison, purely optical approaches, such as FMT, attain spatial resolutions on the order of 1 mm in mice. The strong absorption peak near 800 nm provided by the NIR dye enables MSOT to distinguish dPGS-NIR from the tissue background by statistical means (ICA). Endogenous hemoglobin contrast provides anatomical reference information that can be used to distinguish between signals originating in the injured myocardium from other regions, such as the surgical wound in the thoracic wall.

A further characteristic of the MSOT method as applied here is the high temporal resolution. Parallel detection of optoacoustic signals provided high-rate imaging: each image frame was acquired in less than 40 microseconds whereby the overall frame-rate was defined by the laser pulse repetition at 10 frames per second. Since the individual frames have acquisition times in tens of microseconds, motion blurring on each image collected is

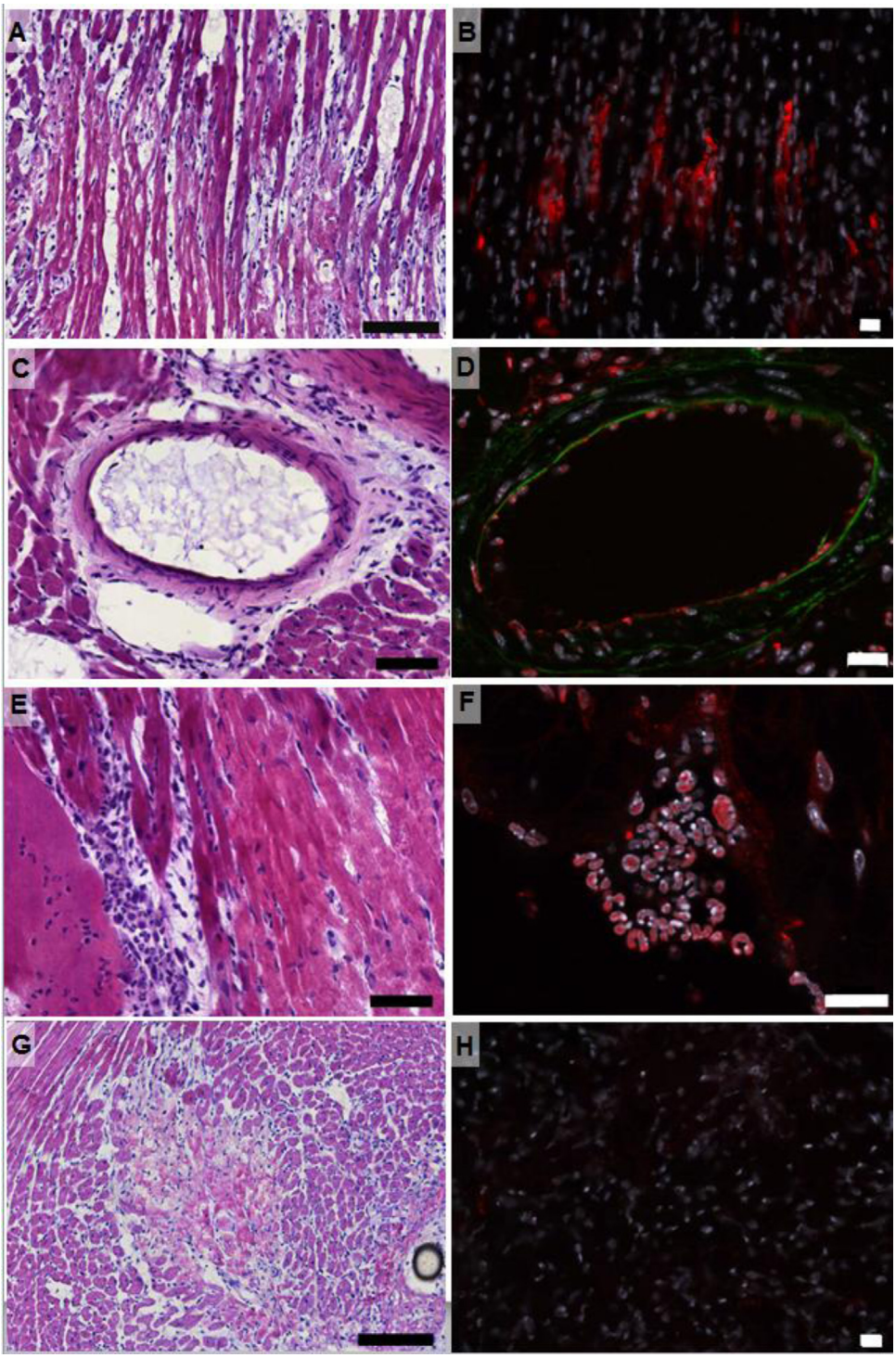

Fig. 4. Histological validation using dPGS-ICC for red emission. (a–f) Animal injected with L- and P-selectin specific dPGS-ICC. (g–h) Animal injected with nonspecific dPG-ICC. (a) Penumbral region of the myocardial infarct, H&E, 200x. Scale bar 100 μm. (b) dPGS-ICC fluorescence signal in the border region of the myocardial infarct, Fluorescence image, 200×. Scale bar 20 μm. (c) Blood vessel in the myocardium, H&E, 400×. Scale bar 50 μm. (d) Fluorescence image of a blood vessel in the myocardium, 400× magnification, showing dPSG-ICC signal originating from endothelial cells. (e) Infiltration of leukocytes into the infarcted area, H&E, 400×. Scale bar 50 μm. (f) dPGS-ICC signal originating from leukocytes, Fluorescence image, 630×. Scale bar 20 μm. (g) Border region of the myocardial infarct, H&E, 200×. Scale bar 100 μm. (h) dPG-ICC fluorescence signal in the border region of the myocardial infarct, Fluorescence image, 200×. The nonspecific agent shows insignificant accumulation compared to dPGS-ICC.

significantly reduced. For a typical heart rate of 10 beats per second, each frame only captures signals from less than 1/2000 of the heart's periodic cycle and an even smaller part of the respiratory cycle. When multiple frames were averaged, inter-frame motion blurring was reduced by grouping frames from similar phases of motion. The imaging protocol applied in this study captured 100 frames at each of 8 wavelengths, resulting in a total acquisition time of 80 s per multispectral 2D slice. In the case of dPGS-NIR, imaging at multiple time points after injection can provide information on the kinetics of the agent.

The histological validation revealed accumulation of dPGS consistent with the expression profiles of P- and L-selectin previously reported [24,25]. Activated leukocytes express L-selectin during various inflammatory conditions, enabling their

extravasation from the circulation into the target tissue *via* the leukocyte adhesion molecule cascade. Correspondingly, activated endothelial cells require P-selectin to recruit leukocytes. Leukocytes recruited to the site of infarction, as well as endothelial cells within the infarcted region, displayed dPGS-ICC signals. This inflammation targeting is consistent with previous reports of dPGS affinity to P- and L-selectins in inflammatory [17] and diagnostic imaging applications [18] for arthritis. A nonspecific control agent devoid of sulfate functions responsible for selectin affinity did not show accumulation in the infarct area.

MSOT demonstrated sufficient sensitivity to detect dPGS in the myocardial infarct. From calibrated NIRF measurements (characterization not shown), we estimate the concentration of dPGS-NIR in the region of myocardial infarction to be in the range of 50–100 μg/ml. Potentially, MSOT contrast can be increased in general by adding multiple dyes to each targeting ligand as in this work, or by employing strongly light-absorbing nanoparticles such as carbon nanotubes [26] or gold nanospheres [12].

A limitation of the current MSOT implementation is that only one 2D slice can be imaged at one time. Quantification of signals in the volume of the myocardium would be more accurate in a true 3D geometry, where a volume of interest would be imaged with an isotropic spatial resolution for each laser pulse. Such systems, which are under development, will require more transducer elements and therefore increased acquisition complexity and processing power.

In summary, we have shown that MSOT in combination with an exogenous optical agent is capable of *in vivo* imaging of myocardial infarction in mice at high resolutions that are not degraded by the strong scattering of light in tissue. This and related approaches have potential practical applications in preclinical research. Small animal studies of myocardial infarction could apply MSOT together with targeted agents to further investigate biological processes during myocardial healing *in vivo* and to evaluate novel therapeutic strategies. Biomarkers in other conditions such as atherosclerosis, arthritis or cancer could be studied by the same technique. MSOT imaging could eventually find diverse use in clinical settings. Potential applications include the examination of inflammation in atherosclerotic plaques in relatively superficial arteries, or *via* an intravascular imaging approach.

Relationship with industry

K.L. has a commercial interest in mivenion GmbH on imaging agent with patent WO2011/095311. V.N. is an equity holder in iThera Medical GmbH.

Funding sources

M.W. is funded by the Kommission für Klinische Forschung der TU München. A.W. is funded by the Deutsche Forschungsgemeinschaft (DFG – German Research Foundation) SFB 824. V.N. is funded by an Advanced Investigator Grant from the European Research Council (ERC).

References

[1] Jaffer FA, Vinegoni C, John MC, Aikawa E, Gold HK, Finn AV, Ntziachristos V, Libby P, Weissleder R. Real-time catheter molecular sensing of inflammation in proteolytically active atherosclerosis. Circulation 2008;118:1802–9.
[2] Jaffer FA, Calfon MA, Rosenthal A, Mallas G, Razansky RN, Mauskapf A, Weissleder R, Libby P, Ntziachristos V. Two-dimensional intravascular near-infrared fluorescence molecular imaging of inflammation in atherosclerosis and stent-induced vascular injury. Journal of the American College of Cardiology 2011;57:2516–26.
[3] Sosnovik DE, Nahrendorf M, Deliolanis N, Novikov M, Aikawa E, Josephson L, Rosenzweig A, Weissleder R, Ntziachristos V. Fluorescence tomography and magnetic resonance imaging of myocardial macrophage infiltration in infarcted myocardium in vivo. Circulation 2007;115:1384.
[4] Swirski FK, Nahrendorf M, Etzrodt M, Wildgruber M, Cortez-Retamozo V, Panizzi P, Figueiredo JL, Kohler RH, Chudnovskiy A, Waterman P. Identification of splenic reservoir monocytes and their deployment to inflammatory sites. Science 2009;325:612.
[5] Ntziachristos V. Going deeper than microscopy: the optical imaging frontier in biology. Nature Methods 2010;7:603–14.
[6] Razansky D, Distel M, Vinegoni C, Ma R, Perrimon N, Koster RW, Ntziachristos V. Multispectral opto-acoustic tomography of deep-seated fluorescent proteins in vivo. Nature Photonics 2009;3:412–7.
[7] Li ML, Oh JT, Xie X, Ku G, Wang W, Li C, Lungu G, Stoica G, Wang LV. Simultaneous molecular and hypoxia imaging of brain tumors in vivo using spectroscopic photoacoustic tomography. Proceedings of the IEEE 2008;96:481–9.
[8] Ntziachristos V, Razansky D. Molecular imaging by means of multispectral optoacoustic tomography (MSOT). Chemical Reviews 2010;110:2783–94.
[9] Herzog E, Taruttis A, Beziere N, Luttich AA, Razansky D, Ntziachristos V. Optical imaging of cancer heterogeneity with multispectral optoacoustic tomography. Radiology 2012;263(2):461–8. doi: 10.1148/radiol.11111646.
[10] Taruttis A, Morscher S, Burton NC, Razansky D, Ntziachristos V. Fast multispectral optoacoustic tomography (MSOT) for dynamic imaging of pharmacokinetics and biodistribution in multiple organs. PLoS ONE 2012;7:e30491.
[11] Eghtedari M, Oraevsky A, Copland JA, Kotov NA, Conjusteau A, Motamedi M. High sensitivity of in vivo detection of gold nanorods using a laser optoacoustic imaging system. Nano Letters 2007;7:1914–8.
[12] Mallidi S, Larson T, Tam J, Joshi PP, Karpiouk A, Sokolov K, Emelianov S. Multiwavelength photoacoustic imaging and plasmon resonance coupling of gold nanoparticles for selective detection of cancer. Nano Letters 2009;9:2825–31.
[13] Taruttis A, Herzog E, Razansky D, Ntziachristos V. Real-time imaging of cardiovascular dynamics and circulating gold nanorods with multispectral optoacoustic tomography. Optics Express 2010;18:19592–602.
[14] Taruttis A, Claussen J, Razansky D, Ntziachristos V. Motion clustering for deblurring multispectral optoacoustic tomography images of the mouse heart. Journal of Biomedical Optics 2012;17:016009.
[15] Razansky D, Harlaar NJ, Hillebrands JL, Taruttis A, Herzog E, Zeebregts CJ, van Dam GM, Ntziachristos V. Multispectral optoacoustic tomography of matrix metalloproteinase activity in vulnerable human carotid plaques. Molecular Imaging and Biology 2011 [Epub ahead of print].
[16] Holotta M, Grossauer H, Kremser C, Torbica P, Volkl J, Degenhart G, Esterhammer R, Nuster R, Paltauf G, Jaschke W. Photoacoustic tomography of ex vivo mouse hearts with myocardial infarction. Journal of Biomedical Optics 2011;16:036007.
[17] Dernedde J, Rausch A, Weinhart M, Enders S, Tauber R, Licha K, Schirner M, Zugel U, von Bonin A, Haag R. Dendritic polyglycerol sulfates as multivalent inhibitors of inflammation. Proceedings of the National Academy of Sciences of the United States of America 2010;107:19679–84.
[18] Licha K, Welker P, Weinhart M, Wegner N, Kern S, Reichert S, Gemeinhardt I, Weissbach C, Ebert B, Haag R, Schirner M. Fluorescence imaging with multifunctional polyglycerol sulfates: Novel polymeric near-IR probes targeting inflammation. Bioconjugate Chemistry 2011;22:2453–60.
[19] Buehler A, Herzog E, Razansky D, Ntziachristos V. Video rate optoacoustic tomography of mouse kidney perfusion. Optics Letters 2010;35:2475–7.
[20] Frangogiannis NG, Smith CW, Entman ML. The inflammatory response in myocardial infarction. Cardiovascular Research 2002;53:31–47.
[21] Nahrendorf M, Swirski FK, Aikawa E, Stangenberg L, Wurdinger T, Figueiredo JL, Libby P, Weissleder R, Pittet MJ. The healing myocardium sequentially mobilizes two monocyte subsets with divergent and complementary functions. Journal of Experimental Medicine 2007;204:3037–47.
[22] Glatz J, Deliolanis NC, Buehler A, Razansky D, Ntziachristos V. Blind source unmixing in multi-spectral optoacoustic tomography. Optics Express 2011;19:3175–84.
[23] Sarantopoulos A, Themelis G, Ntziachristos V. Imaging the bio-distribution of fluorescent probes using multispectral epi-illumination cryoslicing imaging. Molecular Imaging and Biology 2011;13:874–85.
[24] Ley K, Laudanna C, Cybulsky MI, Nourshargh S. Getting to the site of inflammation: The leukocyte adhesion cascade updated. Nature Reviews Immunology 2007;7:678–89.
[25] Venturi GM, Tu L, Kadono T, Khan AI, Fujimoto Y, Oshel P, Bock CB, Miller AS, Albrecht RM, Kubes P, Steeber DA, Tedder TF. Leukocyte migration is regulated by l-selectin endoproteolytic release. Immunity 2003;19:713–24.
[26] De La Zerda A, Zavaleta C, Keren S, Vaithilingam S, Bodapati S, Liu Z, Levi J, Smith BR, Ma TJ, Oralkan O. Carbon nanotubes as photoacoustic molecular imaging agents in living mice. Nature Nanotechnology 2008;3:557–62.